ISSN: 1231-4005
e-ISSN: 2354-0133
DOI: 10.5604/01.3001.0012.2867

DETAILED MODELLING OF THE INTERNAL PROCESSES OF AN INJECTOR FOR COMMON RAIL SYSTEMS

Máté Zöldy, Sándor Vass

Budapest University of Technology and Economics
Department of Automotive Technologies
Stoczek Street 6, 1111 Budapest, Hungary
tel.:+36 1 4632607, +36 1 4632380
e-mail: mate.zoldy@gjt.bme.hu
sandor.vass@gjt.bme.hu

Abstract

In the last few decades exhaust emissions of road vehicles have decreased dramatically, owing to the more and more stringent emission standards issued by the legislative bodies of different countries, combined with the necessity of cleaner, better performing vehicles from society side. The introduction of Common Rail (CR) injection systems has been a great step towards achieving this target, thanks to its flexibility in fuel injection pressure, timing, and length, along variable engine load conditions. However, it is highly time and resource consuming to set up the injection system for all operating points of different engines, moreover, as the injection is a small scale, high speed process, the behaviour of the internal processes is challenging to measure. The best solution for these problems is to create a detailed model of the injector, where all the hydraulic, mechanic, and electromagnetic subsystems are represented, this way the internal working conditions can be analysed and resources can be saved.

In this work, a detailed model of a first generation CR injector for commercial vehicles is presented and validated against needle lift data. The fluid dynamic and mechanic sub-systems are presented in details to thoroughly investigate the working principles of the injector internal parts. The fluid dynamic subsystem contains the chambers, holes, and throttles of the injector, while the mechanic subsystem models the motion and behaviour of the internal parts. The main features of the injector internal working conditions are described and analysed. Apart from the needle lift, these included solenoid anchor, pin and control piston lifts, the control chamber pressure and the mechanical force acting on the anchor. Five test cases were chosen on a medium duty test engine to represent a wide range of operation points from full load to idle and the simulated results were compared to the measured data. The simulated control piston movement accurately matched the measured curves in every test case.

Keywords: *Common Rail, injector, simulation, modelling, internal combustion engines*

1. Introduction

The introduction of Common Rail (CR) injection systems has been a great step towards achieving this target, thanks to its flexibility in fuel injection pressure, timing, and length, along variable engine load conditions [1-3]. The most innovative feature of the CR systems is that they separate the pressure generation physically from the fuel metering. Due to this architecture, the injection is independent from the engine speed or the instantaneous engine load, thus avoiding injection pressure drop at low speeds and loads, as it was the particularity of conventional injection systems [4]. This independence, coupled with the possibility of multiple injections, allows more control over the combustion process, hence it mostly depends on the air-fuel mixing process during and after the injection event [5]. However, it is highly time and resource consuming to set up the system for all operating points of different engines. Moreover, as the injection is a small scale, high-speed process, the behaviour of the internal processes is challenging to measure. The best solution for these problems is to create a detailed model of the injector, where all the hydraulic, mechanic, and electromagnetic subsystems are represented, this way the internal working conditions can be analysed and both time and money can be saved.

As CR systems spread in the market, many CR injector models appeared in the literature. Few attempts have been made to model the whole injection system, including high-pressure pump and rail pipes [6-7], but most models concentrated only on the key part of the system, the injector itself. A couple of simplified models have been made with control purpose [8-9], but most of the works describe the injector processes detailed. Often these models included only two sub-models: a mechanical and a fluid dynamical one [10-16]. Less effort has been spent on modelling the electromagnetic circuit of the solenoid. Among these, the work of Binachi et al. has to be highlighted [17-20], as a complete, detailed, and validated CR injector model under continuous development. Models, which do not contain this sub-model, usually use an interpolation of force data acting on the anchor, defined by measurements [21-22].

The mechanical aspects of injectors have been thoroughly investigated in almost every work, including the elastic axial deformation of the needle and control piston along with the injector body [23], which affects the effective needle displacement and the needle-seat passage area at the orifice holes. Even radial deformation has been modelled to analyse the leakage flow rate [19].

Fluid dynamics is the key factor of CR injector modelling. Most of the models contain some kind of a cavitation modelling. It it crucially affects the discharge coefficient of the orifices and because of this cannot be neglected. Much emphasize was put on determining and describing this phenomenon occurring in various orifices of a CR injector [24]. Along with cavitation, the determination of the discharge coefficient is very critical, because it determines the needle dynamics and the nozzle mass flow rate. The model created by [11] was a rather simple solution, but it proved that the phenomenon of the pressure wave propagation could be used to increase pressure locally in the accumulation chamber of the injector needle, thus increasing injection pressure.

Considering the simulation environment, most models were set up in Matlab/Simulink, [7] and [15] used AMESim code and only a fraction of the available literature set a model up in GT-Fuel [25-26].

The description above showed that a CR injector employs three main sub-models. An electrical, a hydraulic, and a mechanic part needs to be set up in order to describe and investigate all the phenomena that govern injector operation. Before this hybrid architecture could be used as a predictive model of the given injector, it is fundamental to validate the calculated processes in the whole range of possible operation points. In the following chapters, every sub-model made on the basis of a Bosch CRIN1 CR injector for commercial vehicles will be thoroughly presented and a detailed analysis will be given of the working principles and parameter effects.

2. The modelled injector

The Bosch CRIN1 type CR fuel injector was used as a basis to set up the model. The cross section of the injector can be seen on Fig. 1.

The injector consists of five main parts; these together with a few other important components can be followed on Fig. 1. The largest part is the injector body (1); it holds together the multi-hole, valve covered orifice (VCO) type nozzle (2) with the solenoid coil assembly (3) and contains the ball valve body (4). The armature of the solenoid (5) moves together with a steel ball, which is responsible for the opening and closing of the so-called A-throttle. The valve body has two calibrated orifices (A- and Z-throttles) controlling pressure in the control chamber (6) above the corresponding control piston (7). The control piston is in direct physical connection with the nozzle needle (8), which is held down by a needle spring. The high-pressure side of the injector is indicated with red, while the fuel-return with a yellow colour.

Before detailing the model, the working principle of the injector shall be described. It is based on a simple, but clever servo-like mechanism, the hearth of which is the control chamber with the two calibrated orifice. When the system is at rest, the internal ducts, the control chamber and the accumulation volume is filled up by high-pressure oil from the rail pipe. The pressure in the

control chamber with the additional force of the needle spring pushes down the injector needle onto its seat, there is no injection. When the coil of the solenoid is excited, the arising magnetic force pulls up the anchor and opens the ball valve above the control chamber. This way the A-throttle is opened; pressure in the chamber starts to decrease. The Z-throttle is designed to maintain a continuous pressure drop from rail pressure, so during the time when the ball valve is opened, the pressure in the control chamber remains low. On the other side of the assembly, in the accumulation chamber the rail pressure pushes up the needle against the spring and opens the nozzle orifices, the injection begins. When the excitement of the solenoid is finished, the anchor spring closes the ball vale, and the control chamber is filled up again with rail pressure, the control piston pushes down the needle onto its seat and the injection is finished. This process will be analysed more deeply in the chapters below, because many details can influence the procedure.

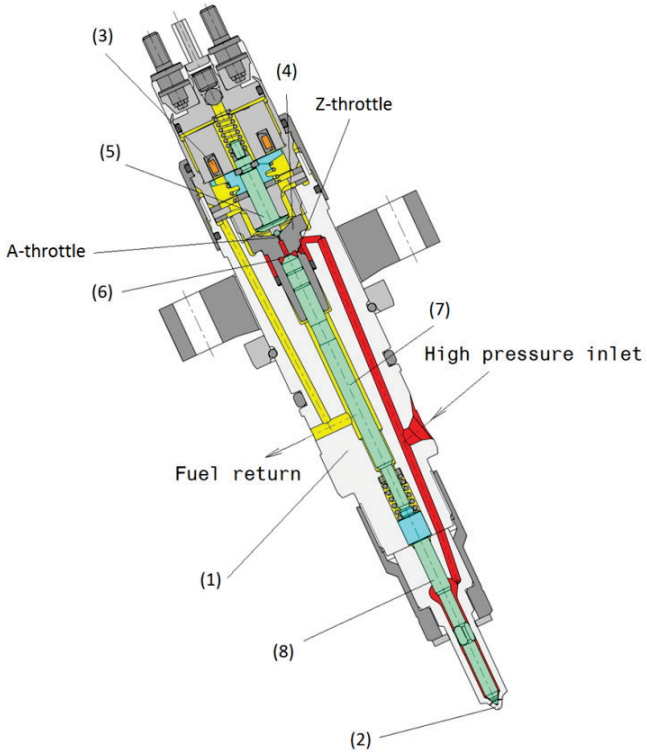

Fig. 1. Cross section of the Bosch CRIN1 injector

3. The modelled injector

An electro-fluid-mechanical hybrid model was set up in order to study the behaviour of a first generation CR injector for commercial vehicles. Although the structure was presented in [27], a deeper analysis and verification was needed to make it predictive. The model was implemented in a commercial simulation software named GT-Suite, in the GT-Fuel submodule. The software is capable of handling different disciplines of physics, such like electromechanical, thermal, fluid-dynamical, and mechanical problems [28]. The governing equations and the build-up of the model will be discussed thoroughly below.

3.1. Electromagnetic model

The electromagnetic model of the solenoid valve is a crucial part of the injector: it is the assembly, which transforms the input current to mechanical force through magnetic circuits.

As mentioned, the output of the electromagnetic subsystem has to be the magnetic force acting on the anchor of the solenoid. This force will be considered by the mechanical sub-model and anchor dynamics will be calculated according to its value. The magnetic force is calculated based on the reluctance of the circuit, when current begins to flow in the coil, magnetic flux flows through the elements and electromagnetic force will be generated between the surfaces of the air gaps. A detailed explanation of the build-up and working principles can be found in [29].

3.2. Hydraulic model

The hydraulic model strictly follows system layout. Modelled parts are connecting pipe between rail tube and injector, internal flow passages of the injector itself; rail tube and high-pressure pump are beyond the scope of this work. Effect of the absence of these parts is eliminated by an unsteady input boundary condition of measured rail pressure during injection. Injector unit has been modelled as a network of pipes and chambers connected by orifices. Higher-level components from software model library were used for calculating fuel leakage, mechanical force produced by chamber pressures and flow at the conical end of the needle.

Calculation is based on one-dimensional, unsteady, compressible flow. It takes into account the dynamics of the attached mechanical components and structural heat transfer [30].

Figure 2 and 3 show the hydraulic and mechanical sub-models of the injector. On Fig. 2, the injector body is presented, while Fig. 3 shows the assembly located in the solenoid.

The geometrical parameters needed in fluid-dynamic equations were measured and implemented in the model; the characteristics of the three main orifices can be followed in Tab. 1.

Tab. 1. Geometric parameters of orifices (Dh – diameter of hole, L – length of hole, r – inlet corner radius)

	D_h [µm]	L [mm]	r [µm]
Injector orifice hole	152	1	20
Hole A	268	0.6	65
Hole Z	220	0.47	55

As pressure and temperature can remarkably vary in CR systems, it is important to use accurate fluid properties. In these simulations ISO4113 test oil was used. The density, bulk modulus, and dynamic viscosity curves of this fluid were predefined in the simulation software as functions of pressure and temperature and analytic functions based on least square method were used for interpolation between the points.

3.3. The mechanical model

The mechanical parts that move during injector functioning (i.e. boll valve, control piston, needle) are modelled with the familiar mass-spring-damper scheme. The masses in the simulation environment may translate and experience velocity in x, y and angular directions, the equations are based on Newton's second law and calculated in every coordinate direction.

The sum of forces acting on a body may include viscous, elastic and body forces, or the user can define external forces acting on the different masses.

As Fig. 2 shows, the injector needle in this model is handled as a rigid body, although the high working pressures of the injection system causes appreciable deformation of the parts. Modelling of this phenomenon has a critical importance on the accuracy of the simulation, as will be shown below. To consider the change of the actual needle stroke due to the axial deformation of the needle, the control piston, and the injector body, the spring stiffness of these three elements was reduced to one element. The mass of the control piston was split into two parts and connected by a spring and a damper element. The spring stiffness can defined using the measurements of

a needle lift sensor and a line pressure sensor. The needle lift sensor indicates the control piston stroke change due to deformation, while the force acting on the piston can be obtained from the measured pressure and the piston diameter. This method eliminates the laborious work of defining the stiffness of all different parts one by one and provides accurate results.

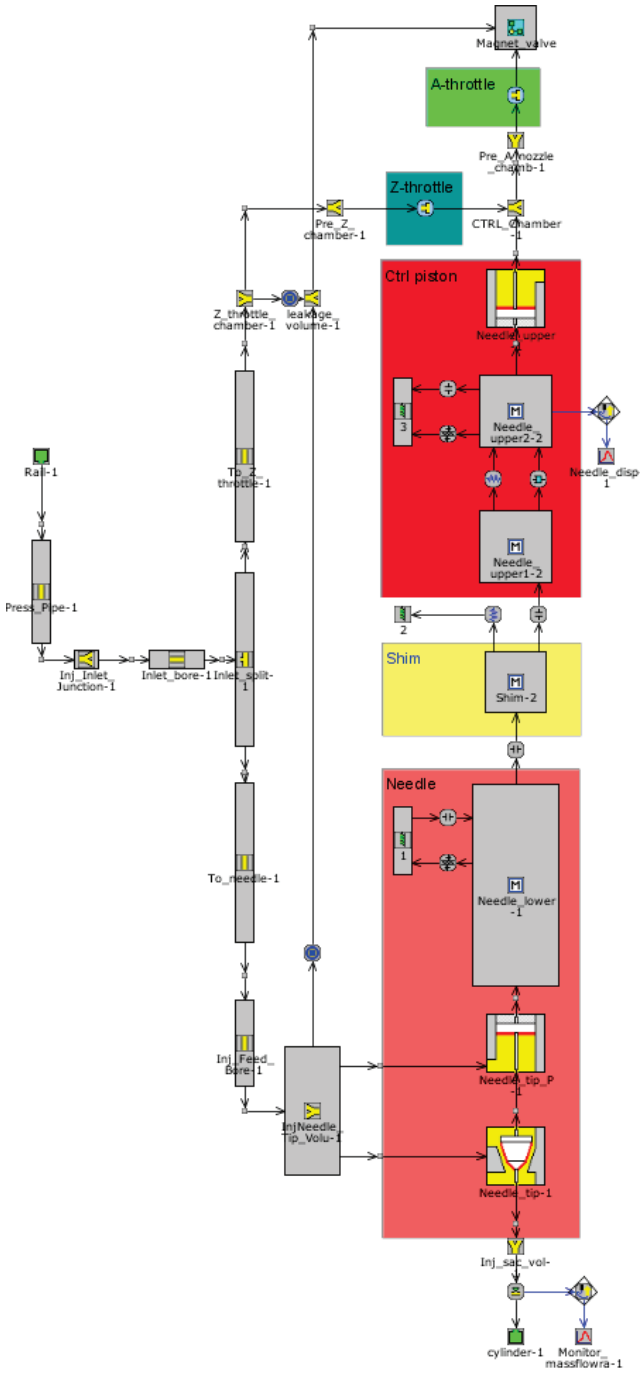

Fig. 2. Hydraulic and mechanical sub-models of the injector body

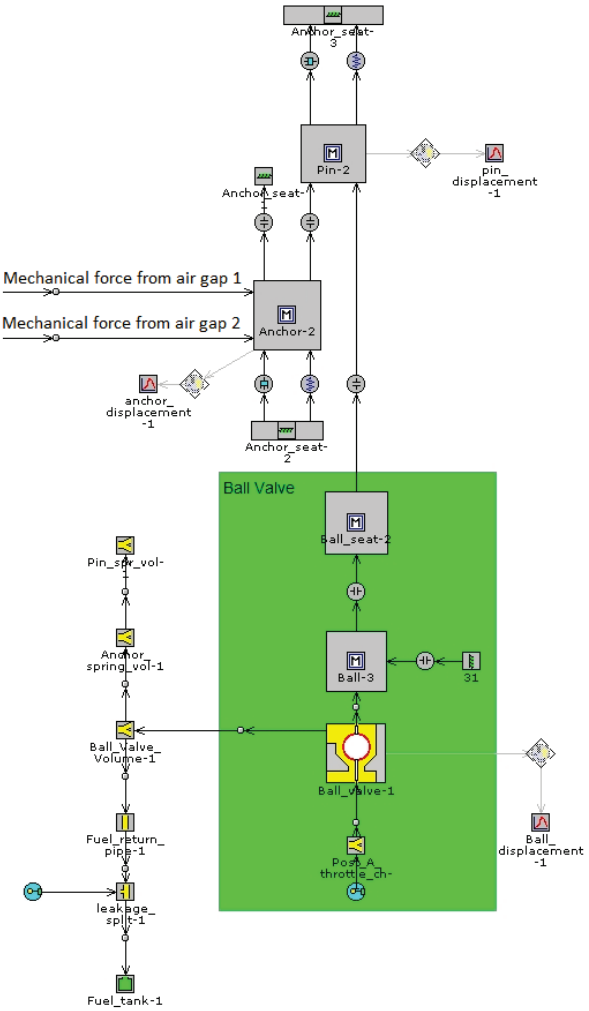

Fig. 3. Hydraulic and mechanical models of the solenoid assembly

The measurement of the masses and springs in the system is relatively easy, but the evaluation of the damping factors is considerably more difficult. Considering e.g. the control piston or the needle, the damping factor shall contain the damping effects of the oil viscosity and the friction between the piston and the liner. Unfortunately, experimental evidences show that the friction component of the damping is much more relevant and it cannot be theoretically evaluated. The

reason for this is that friction is mainly influenced by the machining tolerances; therefore, damping must be estimated during the model-tuning phase.

4. Results and discussion

Results are presented from the comparison of the measured and predicted needle lifts, along with other important parameters covering the whole operating range of the CR system in terms of excitation time and rail pressure, in order to validate the simulation model.

4.1 Test bench layout

The measurements were realized using a four cylinder turbocharged Diesel engine installed on an engine test bench [32]. As Fig. 4 shows, a cylinder head similar to the one on the engine was used to hold the injector.

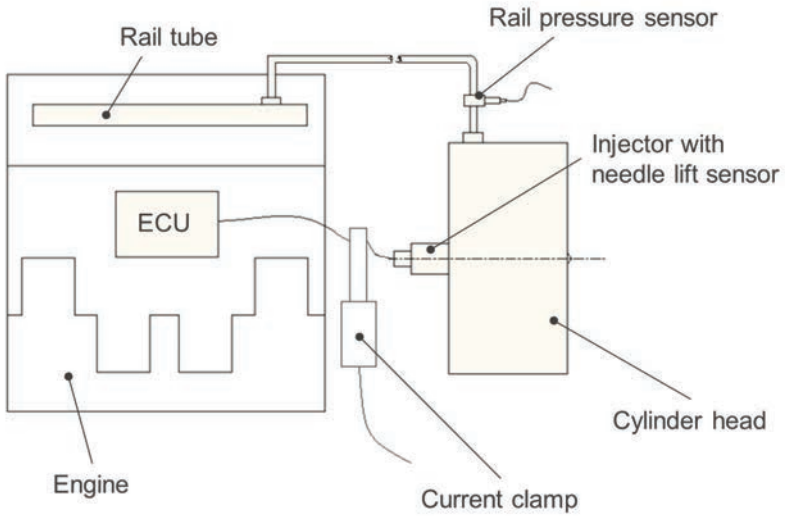

Fig. 4. Test-bench layout

One of the injectors on the engine was disconnected from the rail tube and the ECU. A flexible tube was mounted to provide oil supply to the examined injector, whereas the free electrical connection was used to drive it. This way the engine ran with three cylinders, while the connections of the fourth drove the examined injector.

A current clamp was used to record the driving current and a line pressure sensor was mounted on the rail tube to measure injection pressure. The injector was equipped with a needle lift senor measuring the control piston position, this way all important operation conditions could be monitored except for the injection rate.

Different injection pressures and excitation times were reached by setting different engine operation points on the test bench from full load to idle.

Injections occurred in a stainless steel tube, the pressure of which was maintained at constant 5 bar.

4.2 Test cases, boundary conditions

Five different test cases are presented in this work with five different engine-operating points. The engine speeds, loads and the corresponding measured injection pressures and excitation times can be followed on Tab. 2.

Tab. 2. Test case parameters

Test case	Engine speed [Rpm]	Engine torque [Nm]	Injection pressure [bar]	Excitation time [ms]
1	1400	400	890	2.7
2	1500	300	680	2.55
3	1500	200	540	1.9
4	1500	100	450	1.15
5	900	0	355	0.4 + 0.6

Test case 1 represents full engine load, test cases 2 to 4 represent partial load, while test case 5 was a high idle operational point.

The measured injector current and rail pressure traces were used as inputs for the simulations. This means that the rail pressure was not a constant value, the pressure fluctuation caused by the high-pressure pump and the other injectors were considered in the model. The measured injector currents are shown on Fig. 5.

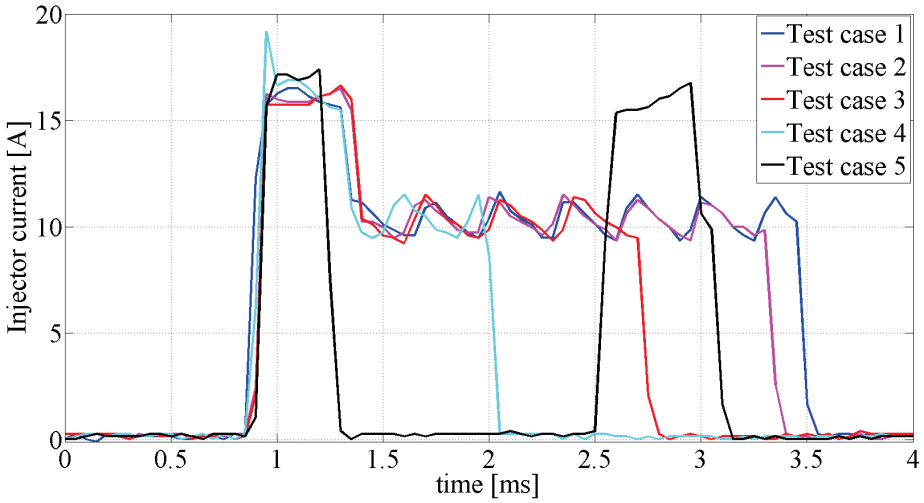

Fig. 5. Injector currents in the different test cases

4.3 Validation and results

The model has been validated by comparisons with measurements in terms of injector control piston lift. Needle lift could not be directly measured, the sensor recorded control piston position.

Five experimental cases cover a wide range of the injector operational domain with different rail pressures and opening times. Four of the five cases represent single injections without pre or post phases, while case 5 shows an operational point at engine idle, with two short injections, low rail pressure, and a needle in ballistic range. Control piston lifts of the first four cases can be followed on Fig. 6; here blue lines represent the measured curves and green lines the simulated ones.

Effect of axial deformation of the control piston and needle is obvious on these position traces. Case 1 has the largest stroke, because rail pressure is the highest here and along with the rail pressure the axial force increases. It is worth noticing that stroke difference reaches 40 µm between cases 1 and 4. It is also worthwhile to point out the ‘humps’ at the beginning of every needle lift. This is caused by the sudden pressure drop when the ball valve opens the control chamber and the control piston expands axially before the actual movement begins. This effect is confirmed when examining the predicted control chamber pressure trace on Fig. 9 and the control piston and needle lifts on Fig. 10. This spring-like behaviour causes the slight delay between the control piston and needle lifts as well.

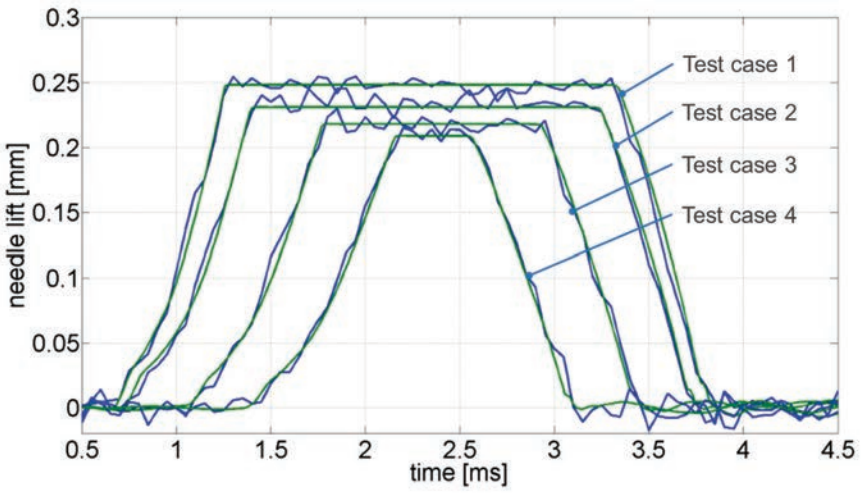

Fig. 6. Measured and simulated control piston lifts for test cases 1 to 4 (measured: blue; simulated: green)

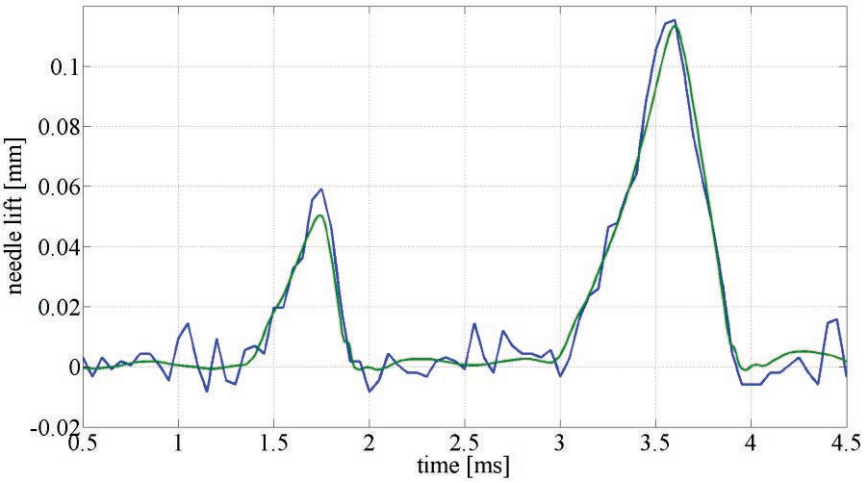

Fig. 7. Measured and simulated control piston lifts for test case 5 (measured: blue; simulated: green)

The control piston lift of case 5 is shown separately from the first four, for visibility reasons. On Fig. 7, the ballistic motion of the control piston of the last case is depicted. The needle does not reach its full stroke neither in the pre nor in the main injection phase.

In all cases, a certain amount of noise can be noticed, but it stays in a tolerable range, so no filtering was used. This way the time shift of the filter was avoided and results that are more accurate could be provided.

All simulations follow the measured traces with good accuracy. To calculate this accuracy, the root mean square (RMS) errors were calculated for every case based on the following equation:

$$\varepsilon_i = \sqrt{\frac{1}{T}\int_0^T \left(\frac{l_{i,meas} - l_{i,sim}}{l_{i,meas}}\right)^2} \quad , \tag{1}$$

where:

ε_i – RMS error,
T – simulation time range,
$l_{i,meas}$ – measured control piston lift,
$l_{i,sim}$ – simulated control piston lift.

The RMS values are presented in Tab. 3.

All RMS error values are less than 1%, so based on Fig. 6 and 7 with the results shown in Tab. 4 it can be stated, that the simulation predicts the needle lifts of the injector very accurately.

Tab. 3. RMS errors

Test case	RMS error
1	0.0053
2	0.0054
3	0.0054
4	0.0054
5	0.0048

The predicted anchor and pin lifts are reported in Fig. 8. Here, like seen in connection with other elements, the pin also suffers a small amount of axial deformation from the preload of the pin spring. It is very small indeed, but when the whole stroke of the assembly is 50 µm, it is noticeable.

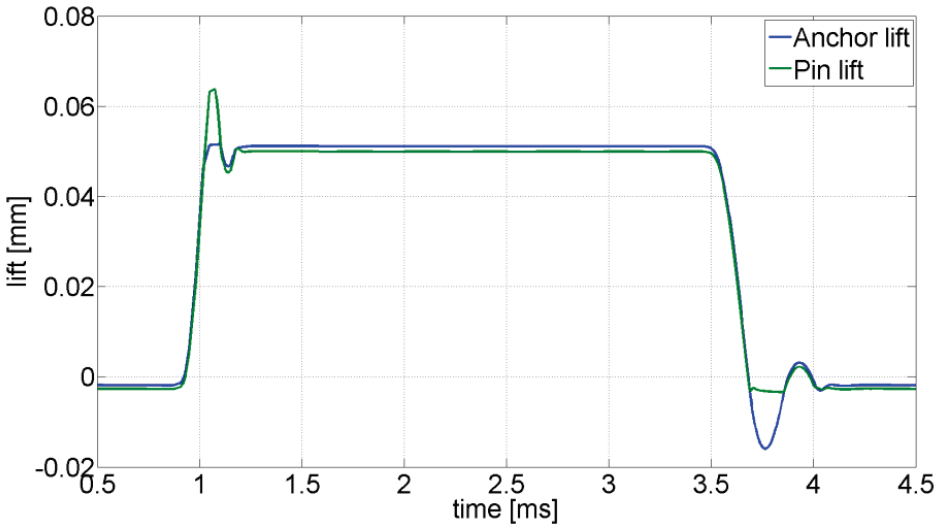

Fig. 8. Predicted anchor and pin lifts for test case 1

Apart from the deformation, the oscillation of the elements can be examined. Initially the anchor and the pin were forming one part, but the weight and eigen frequency of that layout lead to unstable working and high differences in injected masses, due to long oscillation and the re-openings of the control chamber [22]. This was mainly eliminated by separating the anchor and the pin, using an anchor spring to keep the part in place. This build-up gives the ability for the two parts to move separately in one direction. This can be followed on Fig. 8, when the magnetic force opens the ball valve and the anchor reaches full stroke, the pin moves further and bounces back from spring force. When the valve closes, the ball reaches the seat, but the anchor moves further and oscillates back, opening hole A for a moment. This opening can be followed on Fig. 9 as well, where between 3.6 and 4 ms a second, smaller pressure drop appears.

Examining the depicted pressure trace of the control chamber, the two transient processes at the opening and closing shall be analysed more closely. When the ball lifts off the seat, the chamber pressure drops rapidly and the control piston extends along with the needle. Synchronously with this process, the piston starts to move up, opening the needle orifices. As these movements occur, the volume of the control chamber is reduced and the pressure in it rises back. This process is called the pumping effect of the opening phase, and here the A hole acts as a choke and slows down the motion. In the closing phase, the above-mentioned oscillation reopens the valve and closing of the needle orifices is slowed down.

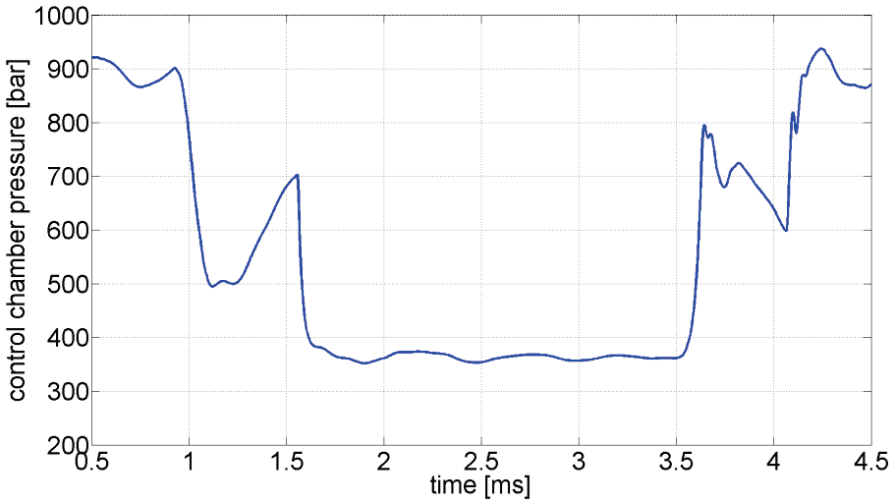

Fig. 9. Predicted control chamber pressure for test case 1

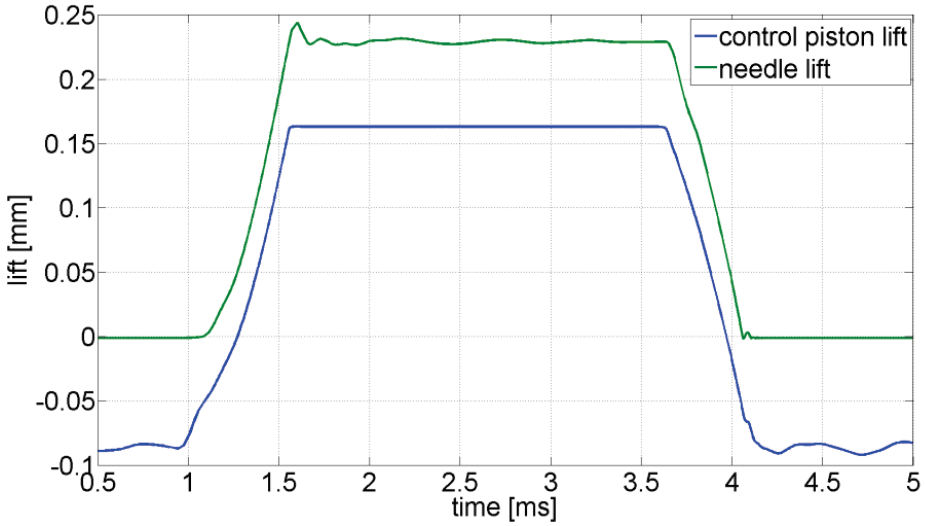

Fig. 10. Predicted control piston and needle lifts for test case 1

On Fig. 10, the deformation of the needle-control piston assembly can be followed. Due to the elastic deformation, the opening of the needle is slightly delayed to the control piston as mentioned before. The full stroke of the piston is about 250 µm, but the needle tip moves less. The reverse process can be observed at the closing phase. The needle reaches its seat first and as the pressure grows back to rail value in the control chamber, the deformation gives extra stroke to the control piston upper end.

5. Conclusion

In this article, a detailed model of a first generation CR injector for commercial vehicles was presented and validated against needle lift data. Five test cases were chosen to represent a wide range of operation points from full load to engine idle. The simulated control piston movement accurately matched the measured curves in every test case.

The fluid dynamic and mechanic sub-systems were presented in details to thoroughly investigate the working principles of the injector internal parts. The main features of the injector internal working conditions were described and analysed.

Validation against injection rate measurements shall be done in the future to make the model fully predictive.

References

[1] Boehner, W., Hummel, K., *Common Rail Injection System for Commercial Diesel Vehicles,* SAE Technical Paper Series 970345, 1997.

[2] Flaig, U., Polach, W., Ziegler, G., *Common Rail System (CR-System) for Passenger Car DI Diesel Engines; Experiences with Applications for Series Production Projects,* SAE Technical Paper Series 1999-01-0191, 1999.

[3] Strumpp, G., Ricco, M. *Common Rail – An Attractive Fuel Injection System for Passenger Car DI Diesel Engines,* SAE Technical Paper Series 960870, 1996.

[4] Zellbeck, H., Schmidt G., *Einspritzsysteme für zukünftige Anforderungen an schnellaufenden Dieselmotor, MTZ* 56(11): 648-655, 1995.

[5] Heywood, J. B. *Internal combustion engine fundamentals*. McGraw-Hill Publishing, New York 1988.

[6] Sabau, A., Barhalescu, M., Oanta, E., *Modelling of high pressure fuel injection systems*, Annals of DAAAM for 2012 & Proceedings of the 23rd International DAAAM Symposium Vol. 23, No. 1, 2011.

[7] Chiavola, O., Giulanelli, P., *Modelling and Simulation of Common rail Systems*, SAE Technical Paper Series 2001-01-3183, 2001.

[8] Lino, P., Maione, B., Rizzo, A., *Nonlinear modelling and control of a common rail injection system for diesel engines,* Applied Mathematical Modelling 31: 1770-1784., 2007.

[9] Palamondon, E., Seers, P., *Development of a simplified dynamic model for a piezoelectric injector using multiple injection strategies with biodiesel / diesel-fuel blends,* Applied Energy 131: 411-424, 2014.

[10] Brusca, S., Giuffrida, A., Lanzafame, R., Corcione, G. E., *Theoretical and experimental analysis of diesel sprays behaviour from multiple injections common rail systems,* SAE Technical Paper Series 2002-01-2777, 2002.

[11] Catalano, L. A., Tondolo, V. A., Dadone, A., *Dynamic rise of pressure in the common rail fuel injection system,* SAE Technical Paper Series 2002-01-0210, 2002.

[12] Digesu, P., Ficarella, A., Laforgia, D., Bruni, G., Ricco, M., *Diesel Electro-Injector: A Numerical Simulation Code,* SAE Technical Paper Series 940193, 1994.

[13] Huhtala, K., Vilenius, M., *Study of a common rail fuel injection system,* SAE Technical Paper Series 2001-01-3184, 2001.

[14] Mulemane, A., Han, J-S., Lu P-H., Yoon, S-J., Lai, M-Ch., *Modelling Dynamic Behavior of Diesel Fuel Injection Systems,* SAE Technical Paper Series 2004-01-0536, 2004.

[15] Payri, R., Climent, H., Salvador, F. J., Favennec, A. G., *Diesel injection system modelling. methodology and application for a first-generation common rail system,* Proceedings of the Institution of Mechanical Engineering Vol. 218, Part D, 2004.

[16] Bereczky A, Lukács K., *Development of Dual fuel engine and modelling of it with AVL Boost software system* In: Stanislaw Szwaja (szerk.) Technologia uprawy mikroglonów w bioreaktorach zamkniętych z recyklingiem CO2 i innych odpadów z biogazowni. Konferencia helye, ideje: Kroczyce, Lengyelország, Instytut Maszyn Cieplnych Polit. Czestochowska, pp. 11-16, Czestochowa 2015.

[17] Bianchi, G. M., Falfari, S., Pelloni P., Filicori, F., Milani, M. *A Numerical and Experimental Study on the Possible Improvements of C.R. Injectors,* SAE Technical Paper Series 2002-01-0500, 2002.

[18] Bianchi, G. M., Falfari, S., Pelloni P., Song-Charng Kong, Reitz, R.D., *Numerical Analysis of High Pressure Fast-Response C.R. Injector Dynamics,* SAE Technical Paper Series 2002-01-0213, 2002.

[19] Bianchi, G. M., Falfari, S., Parotto, M., Osbat, G., *Advanced Modelling of Common Rail Injector Dinamics and Comparison with Experiments,* SAE Technical Paper Series 2003-01-0006, 2003.

[20] Amiola, V., Ficarella, A., Laforgia, D., De Matthaeis, S., Genco, C., *A theoretical code to simulate the behaviour of an electro-injector for diesel engines and parametric analysis,* SAE Technical Paper Series 970349, 1997.
[21] Ficarella, A., Laforgia, D., Landriscina, V., *Evaluation of instability phenomena in a common rail injection system for high speed diesel engines*, SAE Technical Paper Series 1999-01-0192, 1999.
[22] Dongiovanni, C., Coppo, M., *Accurate Modelling of an Injector for Common Rail Systems,* Fuel Injection, InTech, ISBN: 978-953-307-116-9, 2010.
[23] Von Kunsberg Sarre, C., Kong, S-C., Reitz, R. D., *Modelling the Effects of Injector Nozzle Geometry on Diesel Sprays,* SAE Technical Paper Series 1999-01-0912, 1999.
[24] Kolade, B., Boghosian, M. E., Reddy, P. S., Gallagher, S., *Development of a General Purpose Thermal- Hydraulic Software and its Application to Fuel Injection Systems,* SAE Technical Paper Series 2003-01-0702, 2003.
[25] Kolade, B., Morel, T., Kong, S-C. *Coupled 1-D/3-D Analysis of Fuel Injection and Diesel Engine Combustion,* SAE Technical Paper Series 2004-01-0928, 2004.
[26] Vass, S., Németh, H. *Sensitivity analysis of instantaneous fuel injection rate determination for detailed Diesel combustion models,* Periodica Polytechnica, Transportation Engineering 41(1): 77-85, 2013.
[27] GT-Suite 7.3.0 User's Manual, Gamma Technologies Inc., 2012.
[28] Vass, S., Németh, H., *Detailed electromagnetic model of a Common Rail injector*, 34th International Colloquium on Advenced Manufacturing and Repairing Technologies in Vehicle Industry, Visegrád, Hungary, pp. 165-168, 2017.
[29] Kolade, B., Boghosian, M. E., Reddy, P.S., Gallagher, S., *Development of a General Purpose Thermal – Hydraulic Software and its Application to Fuel Injection Systems,* SAE Technical Paper Series 2003-01-0702, 2003.
[30] Miller, D. S., *Internal Flow Systems*, BHRA Fluid Engineering, Bedford 1990.
[31] Bárdos, Á., Vass, S., Németh, H., *Validation of a detailed commercial vehicle turbocharged diesel engine model,* A Jövő Járműve 1-2/2014: 25-31, 2014.

Manuscript received 26 March 2018; approved for printing 29 June 2018